energies

MDPI

Article

Time-Varying Characteristics of CH_4 Displacement–Replacement Effect in Coal Seams During CO_2-Enhanced Coalbed Methane Recovery

Jianchi Hao [1,*], Shuangming Wang [1], Hu Wen [2], Zegong Liu [3] and Xuezhao Zheng [2]

[1] College of Geology and Environment, Xi'an University of Science and Technology, Xi'an 710054, China
[2] College of Safety Science and Engineering, Xi'an University of Science and Technology, Xi'an 710054, China
[3] College of Safety Science and Engineering, Anhui University of Science and Technology, Huainan 232002, China
* Correspondence: 13572468308@163.com; Tel.: +86-13572468308

Abstract

Carbon dioxide (CO_2)-enhanced coalbed methane recovery involves a complex process of mixed-gas adsorption, desorption, and diffusion–transport. The literature suggests that an appropriate range of CO_2 injection pressure and an optimal injection time window are critical for coal seams with varying reservoir conditions. That is, higher pressure and longer injection periods do not necessarily lead to better displacement performance. Therefore, in this study, experimental research was conducted on the time-varying characteristics of the displacement–replacement effect of CO_2-enhanced methane (CH_4) extraction from coal seams, and the following results were obtained. (1) The process of displacement–replacement of CH_4 by CO_2 in coal seams can be divided into five stages: a stage of spontaneous CH_4 desorption caused by partial-pressure effects, a replacement-dominated stage, a stage where replacement and displacement act jointly, a displacement-dominated stage, and a stabilization stage. (2) For all three coal samples (anthracite, coking coal, and long-flame coal), cumulative CH_4 desorption increases with increasing CO_2 injection pressure below 5 MPa and finally stabilizes. However, when CO_2 injection pressure exceeds 5 MPa, the effect weakens, possibly due to the dynamic changes in CO_2 partial pressure. (3) The displacement–replacement ratio decreases with increasing CH_4 equilibrium pressure. Additionally, the larger the difference between the CO_2 injection pressure and the CH_4 equilibrium pressure, the better the displacement–replacement effect.

Keywords: gas management; gas extraction; CO_2 adsorption by coal; methane desorption

check for updates

Academic Editor: Dameng Liu

Received: 23 September 2025
Revised: 15 October 2025
Accepted: 16 October 2025
Published: 18 October 2025

Citation: Hao, J.; Wang, S.; Wen, H.; Liu, Z.; Zheng, X. Time-Varying Characteristics of CH_4 Displacement–Replacement Effect in Coal Seams During CO_2-Enhanced Coalbed Methane Recovery. *Energies* **2025**, *18*, 5507. https://doi.org/10.3390/en18205507

Copyright: © 2025 by the authors. Licensee MDPI, Basel, Switzerland. This article is an open access article distributed under the terms and conditions of the Creative Commons Attribution (CC BY) license (https://creativecommons.org/licenses/by/4.0/).

1. Introduction

Coal serves as China's fundamental and backup energy source, playing a deeply integrated role in the country's economy. Coal bed methane (CH_4, CBM) is a valuable, high-quality, and clean resource associated with coal, and its efficient extraction is crucial for preventing and controlling disasters related to its catastrophic explosions, making it an important option and cleaner than conventional fossil fuels [1–4]. China's coal seam structure is complex, with generally low permeability of coal. Shallow coal resources are notably depleting, leading to a shift in coal development to deeper levels, which has now become the norm. The increasingly evident low-permeability characteristics of coal seams, complex geology, and technical limitations have become the bottlenecks, making CH_4 extraction more difficult and increasing the pressure to prevent and control CH_4

disasters [5,6]. Thus, industrial innovation is required to manage hazards and maintain productivity at greater depths. Unfortunately, traditional negative pressure extraction technology cannot overcome the challenge of low permeability in coal seams. Pre-extraction is time consuming and yields slow results, failing to meet the needs of mining succession and underground safety production [7]. To address the challenge of low permeability in coal seams, China has implemented measures such as mining protective layers, hydraulic fracturing/slotting/punching, and loosening blasting to enhance CH_4 drainage and improve coal seam permeability [8]. Although most permeability enhancement measures have successfully improved the permeability of coal seams, the issue of a sharp decline in extraction efficiency due to the decrease in reservoir pressure during the later stages of mining remains unresolved. Therefore, development of a simple and effective new technology to improve coal seam permeability and enhance gas extraction efficiency is urgently demanded [9]. With the continuous advancement of science and technology, breakthroughs have been made in gas injection displacement–replacement technology [10]. The successful experiment of carbon dioxide (CO_2)-enhanced CBM (CO_2-ECBM) recovery via gas injection has provided a new innovative approach to improve underground gas extraction efficiency using gas injection displacement. The injection of CO_2 into the coal seam can not only compete with CH_4 stored in the coal seam for adsorption, reduce the effective partial pressure of the gas, and promote the desorption of adsorbed gas but can also increase the internal pressure of the coal body, enhance the mixed gas percolation velocity, effectively compensate for the reservoir pressure drop during the later stages of extraction, and provide sufficient power and reliable migration pathways for the reservoir flow field [11] (Figure 1). Simultaneously, CO_2 can be stored in the coal seam, which can significantly reduce its greenhouse effect. This technology has attracted tremendous research attention due to its safety, economic feasibility, environmental friendliness, and significant improvement in gas recovery rate, and offers promising application prospects in the near future.

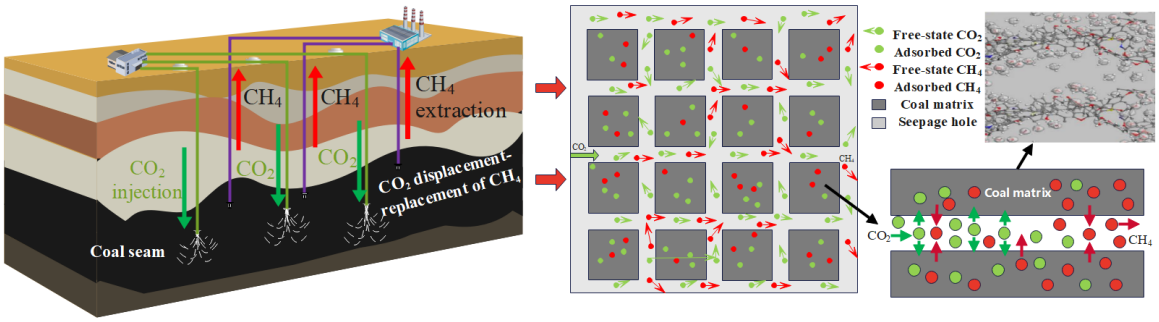

Figure 1. Schematic illustration of CO_2-ECBM recovery mechanism via CO_2 displacement–replacement.

Many researchers have conducted similar experimental research and concluded that displacement and replacement effects occur throughout the gas injection process, but the dominant role varies at different stages [12–14]. Furthermore, several experiments were performed on CO_2 displacement in large-sized coal rock specimens, and it was found that factors such as gas injection pressure, speed, gas content, reservoir structure, and permeability jointly determined the displacement effect [15,16]. For instance, Wang et al. conducted CO_2/N_2 replacement experiments on CBM under different gas injection pressure and stress conditions and analyzed the impact of experimental conditions on the replacement volume ratio and gas breakthrough time [17,18]. Wang et al. used Comsol to compare the stimulation effects of injecting N_2 and CO_2 on CBM displacement, concluding that injecting CO_2 was more effective at increasing CH_4 production than injecting N_2, and

the gas content in the coal seam decreased at a faster rate with the increase in the gas injection pressure [19]. Sun et al. reported that injecting CO_2 not only reduced the partial pressure of CBM and accelerated its desorption but also made the coal body more prone to adsorbing CO_2 gas, which could compete with and adsorb CH_4 molecules in the coal, thereby increasing the production of CBM [20]. Several researchers focused on the technical characteristics of gas injection displacement to enhance the recovery of CBM [21–24]. Based on the percolation equation, diffusion equation, and multi-component gas adsorption equation, they established a coupled equation and introduced practical examples for its solution, deriving the pressure distribution of CBM, gas concentration distribution, and a quantitative relationship between permeability and gas concentration.

Focusing on underground gas control in coal mines, Wen et al. proposed a technique for fracturing coal and rock and displacing coal-seam CH_4 using liquid CO_2 (Figure 2). They designed field tests involving the displacement of coal-seam CH_4 by CO_2, which effectively shortened the pre-drainage time and reduced the drilling workload for drainage boreholes [25–27]. The phase-transition process of liquid CO_2 injected into the coal seam through boreholes is illustrated in Figure 3. In the figure, A–B is liquid-phase pressurization, B–C is fluid–solid heat transfer, C–D is liquid-phase seepage, D–E represents two-phase seepage and diffusion, and E-F is gas-phase adsorption and diffusion. The effectiveness of liquid CO_2 in enhancing coal-seam CH_4 drainage primarily depends on the gas-phase adsorption–diffusion–seepage stage (D–F in Figure 3). This stage involves complex physical processes including gas-phase CO_2 seepage, diffusion, and adsorption, and features multi-field coupling among the temperature field, pressure field, and gas concentration field.

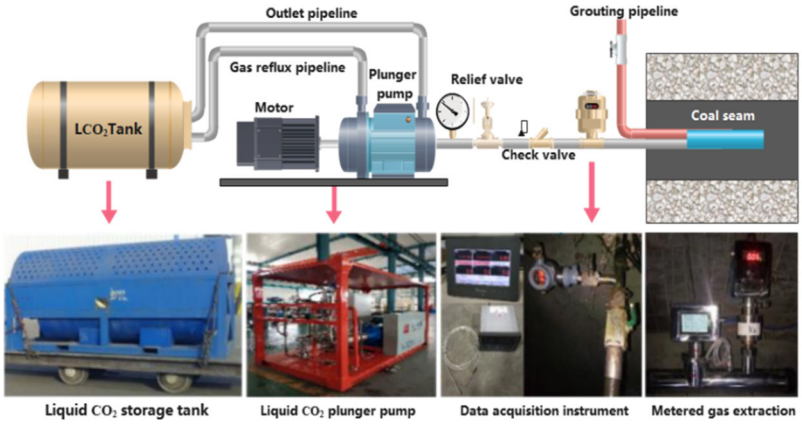

Figure 2. Technological process and equipment for liquid CO_2 displacement of CH_4 in coal seams.

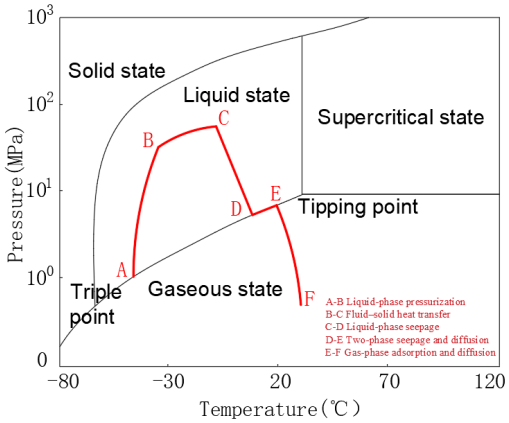

Figure 3. Phase change curve during liquid CO_2 pressure injection process.

After injecting CO_2 into a coal seam, high-pressure gas flow initially carries part of the CH_4 out of the coal, reducing the amount of free CH_4 and weakening the displacement effect. With the continuous diffusion of CO_2 into the coal matrix, the sorption replacement effect begins to act, promoting the desorption and diffusion of adsorbed CH_4. This increases the free CH_4 and simultaneously strengthens the displacement effect. Therefore, compared with the displacement effect, the replacement effect exhibits a clear lag, and the two effects promote and constrain each other through a mutual feedback relationship, which is a key factor influencing CH_4 production. However, currently employed CO_2 displacement–replacement experiments generally analyze only the enhancement of CH_4 recovery, and research on the time-varying characteristics of the displacement and replacement effects is still lacking.

Briefly, CO_2-enhanced CBM (ECBM) recovery is a complex process involving adsorption, desorption, and diffusion–transport of mixed fluids. Studies have shown that, for coal seams under different reservoir conditions, there exists an appropriate range of CO_2 injection pressure and an effective time window. That is, higher pressure and longer injection times do not necessarily yield better displacement performance. Therefore, this study focuses on the following three issues. The current theoretical research on CO_2-enhanced extraction of CH_4 from coal seams remains imperfect, the injection parameters lack scientific guidance, and full enforcement of the displacement effect is difficult. In this study, experimental research was conducted on the time-varying characteristics of the displacement–replacement effect of CO_2-enhanced extraction of CH_4 from coal seams. The results reveal the time-varying characteristics of the dominant position of displacement and replacement effects and aid in determining the key control parameters corresponding to displacement and replacement effects, providing theoretical guidance for optimizing on-site extraction and injection schemes.

2. Experimental Setup and Scheme

The experimental setup integrated a large-bore nuclear magnetic resonance (NMR) imaging analyzer (MacroMR12-150H-I) with a high-pressure gas-injection displacement platform. The main components include an NMR imaging analyzer, a coal sample vessel, pneumatic valves, a gas storage tank, a pressure control unit, temperature sensors, a vacuum pump, and gas cylinders (Figure 4).

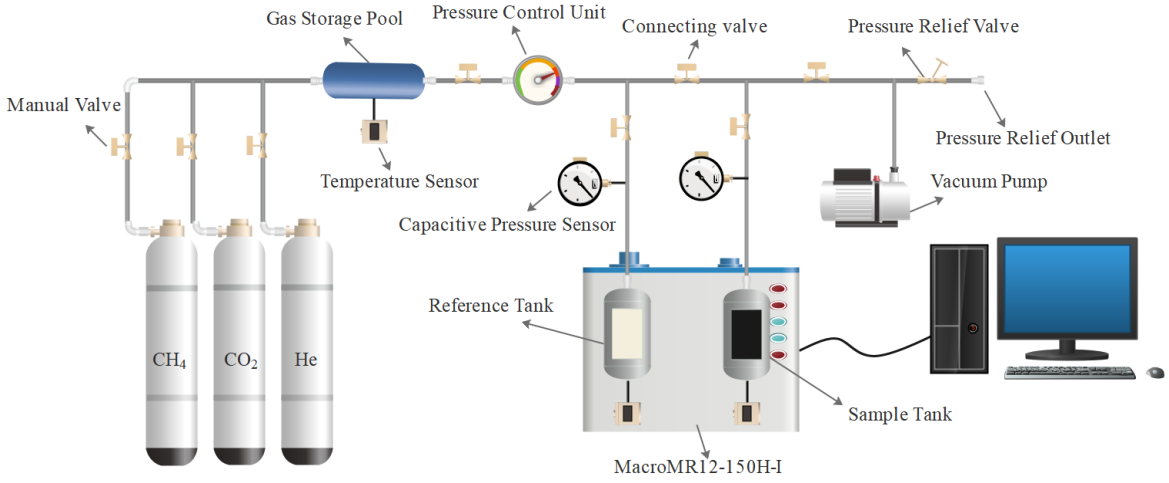

Figure 4. Schematic representation of the experimental system.

2.1. Experimental Principle

During the experiment, the following relationship exists for CH_4 gas:

$$V_{dei(CH_4)} = V_{ad0(CH_4)} - V_{adi(CH_4)} \quad (1)$$

$$V_{freei(CH_4)} = V_{dei(CH_4)} + V_{free0(CH_4)} \quad (2)$$

where $V_{dei(CH_4)}$ is the desorption amount of CH_4, $V_{ad0(CH_4)}$ denotes the initial adsorption capacity of CH_4, $V_{adi(CH_4)}$ is the amount of residual CH_4 adsorption at time i, $V_{freei(CH_4)}$ is the free CH_4 gas volume at time i, and $V_{free0(CH_4)}$ represents the free CH_4 gas volume at the beginning of the experiment.

The partial pressure of free CH_4 gas at the time i is expressed as follows:

$$\mathrm{P_{freei(CH_4)}} = \frac{\mathrm{Zn_{i(CH_4)}RT}}{\mathrm{V_{freei(CH_4)}}} \quad (3)$$

where $\mathrm{P_{freei(CH_4)}}$ is the partial pressure of CH_4 gas in free state at time i, Z denotes the compression factor of the mixture at the experimental temperature, R is the general gas constant, i.e., 8.314 J (mol K), T is the temperature in K, and V_0 denotes the volume of free space.

According to Dalton's partial pressure law, the partial pressure of CO_2 at time i can be obtained as follows:

$$\mathrm{P_{freei(CO_2)}} = \mathrm{P_i} - \mathrm{P_{freei(CH_4)}} \quad (4)$$

Therefore, the amount of free state CO_2 at time i is

$$V_{freei(CO_2)} = \frac{\mathrm{Zn_{i(CO_2)}RT}}{\mathrm{P_{freei(CO_2)}}} \quad (5)$$

Moreover, the amount of adsorbed CO_2 is expressed as follows:

$$V_{ad0(CO_2)} = V_{0(CO_2)} - V_{freei(CO_2)} \quad (6)$$

2.2. Experimental Scheme

Coal samples of anthracite, coking coal, and long-flame coal were selected for the experiments, and they were dried in an oven at 80 °C. First, an NMR CH_4 gas calibration test was conducted at temperatures of 20–60 °C and test pressures of 1–6 MPa. Subsequently, a time-varying experiment was conducted on the displacement–replacement effects of CO_2-enhanced extraction of coal-seam CH_4. The prepared coal samples with dimensions of 100 mm × 50 mm were subjected to coal quality analysis and measurements of true density and apparent density. The mass of the loaded coal sample, free volume of the sample chamber, V_1 = 33.39 mL, and the free volume of the reference tank, V_2 = 44.87 mL, were recorded. The experimental temperature was 20–60 °C, the CH_4 equilibrium pressure was 1–3 MPa, and the CO_2 injection pressure was 2–6 MPa with a step of 1 MPa. Table 1 presents the industrial analysis results of the coal sample.

Table 1. Experimental parameters and corresponding results for the coal cores.

Experimental Parameters	Long Flame Coal	Coking Coal	Anthracite
Moisture/%	5.58	3.15	1.86
Ash/%	12.37	9.95	9.51
Volatile Matter/%	42.28	27.68	16.28
Porosity/%	6.38	6.07	5.76
Bound flow saturation/%	55.7079	50.98	56.093
Free fluid saturation/%	44.4018	49.02	43.906

3. NMR CH_4 Calibration Experiment

Prior to the experiment, the lines were evacuated for 6 h, and then CH_4 was injected into the sample chamber at a pressure of 1–6 MPa to acquire NMR signals under different pressure and temperature conditions. Considering the temperature of 30 °C as a representing example, the T_2 spectrum of free CH_4 was obtained, as shown in Figure 5.

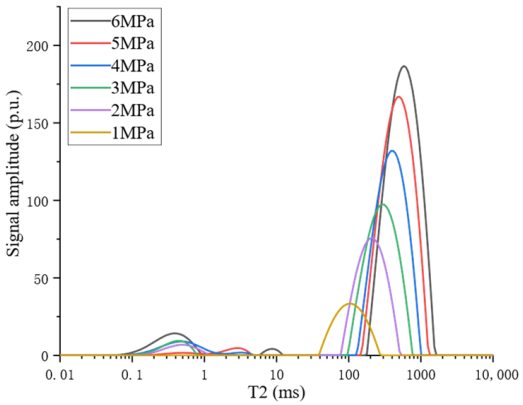

Figure 5. T_2 curve of free state CH_4 peak at 30 °C temperature condition.

The NMR test results of free gas reveal that the T_2 spectrum of free gas exhibits only one characteristic peak, and both the peak area (integral amplitude) and the transverse relaxation time T_2 are proportional to gas pressure. This means that as pressure increases, the peak shifts to longer T_2 (rightward). Therefore, in the NMR spectra of coal gas adsorption/desorption, the spectral ranges corresponding to adsorbed and free gas can be distinguished.

Based on the T_2 spectra of free CH_4, the signal amplitude integration corresponding to free CH_4 at 1–6 MPa was extracted to plot a fitted curve of pressure versus T_2 signal amplitude integrations of free CH_4, as shown in Figure 6. According to natural gas calculation of compression factor [28], the compression factor Z was calculated under different pressures, and the corresponding results are listed in Table 2. Then, the mass of CH_4 under different pressure and temperature conditions was calculated by using the real-gas equation of state PV = ZnRT. Therefore, by this method, the measured relationship between pressure and the T_2 signal amplitude integration of free CH_4 can be converted into a correspondence between CH_4 mass and the T2 signal amplitude integration of free CH_4, as shown in Figure 7.

The results reveal that, at different temperatures, the CH_4 mass is proportional to the integrated signal amplitude of the NMR T_2 spectrum. In other words, the greater the mass of free CH_4, the larger the integrated signal amplitude. The relationship is linear, with coefficients of determination R^2 all exceeding 0.9960. Therefore, by using the fitted curve between the integrated T_2 signal amplitude and CH_4 mass, the CH_4 mass under different pressure conditions can be calculated, thereby completing the calibration of free-state CH_4.

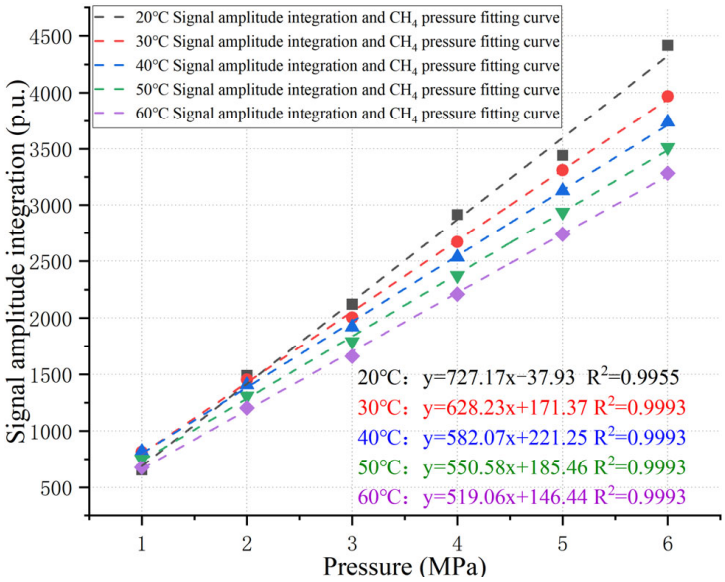

Figure 6. Relationship between pressure and signal amplitude integration.

Table 2. Relationship between compressibility factor Z and methane mass.

Pressure/MPa	Z	CH_4 Mass/g	Amplitude Integral
0.99	0.98	0.2254	656.6120
2.07	0.96	0.4811	1490.8610
2.96	0.94	0.7025	2121.6470
4	0.92	0.9700	2914.1360
4.95	0.9	1.2271	3442.1290
5.95	0.89	1.4915	4417.5120
6.94	0.87	1.7797	5047.4240
7.96	0.86	2.0650	5822.2680

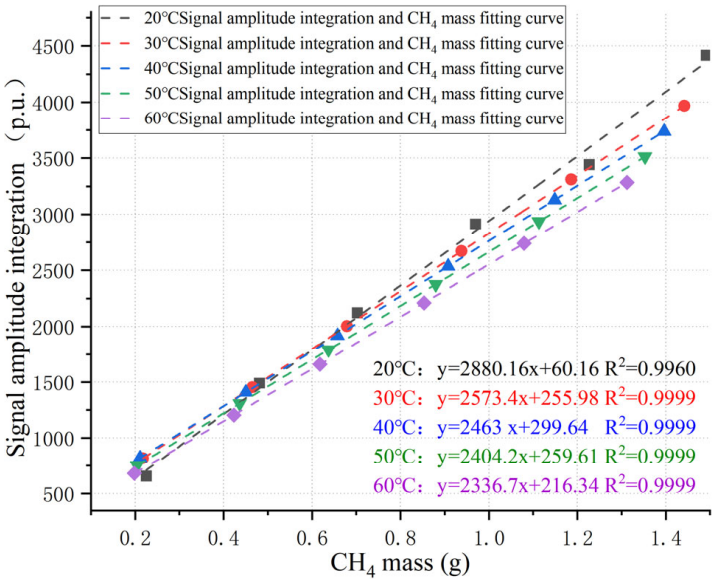

Figure 7. Integral fitting curve of free-state CH_4 mass and signal amplitude integration.

4. Experimental Study on the Time-Varying Characteristics of Displacement–Replacement Effects in CO_2-Enhanced Extraction of Coal-Seam CH_4

Injection of gaseous CO_2 into coal seams to displace and replace CH_4 is a dynamic and complex process. The driving mechanisms that enhance CH_4 drainage differ across injection stages, influenced by both displacement and replacement effects. Throughout the injection process, these two effects dominate at different times and gradually transition from one to the other. These displacement and replacement effects are influenced by CO_2 injection pressure, in situ CH_4 pressure, temperature, and injection duration. A quantitative study of these factors is necessary to establish rational production-enhancement schemes and to select target reservoirs. Therefore, understanding the time-dependent characteristics of displacement–replacement effects, establishing quantitative metrics for CH_4 production from each effect, and identifying the key controlling parameters for each can provide theoretical guidance for optimizing field injection–production strategies.

The coal samples used in the experiments included long-flame coal, coking coal, and anthracite. To calculate the amount of CH_4 desorbed during the CO_2 gas displacement–replacement of CH_4, NMR T_2 spectra were first acquired under each set of conditions. After obtaining the T_2 spectra, the relationship between the integrated T_2 signal amplitude and free-phase CH_4 was used to determine the time evolution of CH_4 desorption. Further, the residual adsorbed CH_4, the adsorbed amount of CO_2, and the amount of free-phase CO_2 were indirectly calculated.

4.1. Effect of CO_2 Injection Pressure

Gaseous CO_2 was injected at pressures of 2–6 MPa by a controlled-variable method, with the CH_4 equilibrium pressure set at 1 MPa and the temperature at 30 °C. The CH_4 desorption per unit time was calculated. By analyzing the time evolution of CH_4-stage desorption amount, the time-varying characteristics of the displacement and replacement effects were elucidated, and the optimal CO_2 injection pressure range was identified.

4.1.1. Time-Varying Characteristics of CH_4-Stage Desorption Amount

The relationships between the CH_4-stage desorption amount and displacement time and CO_2 injection pressure are shown in Figure 8.

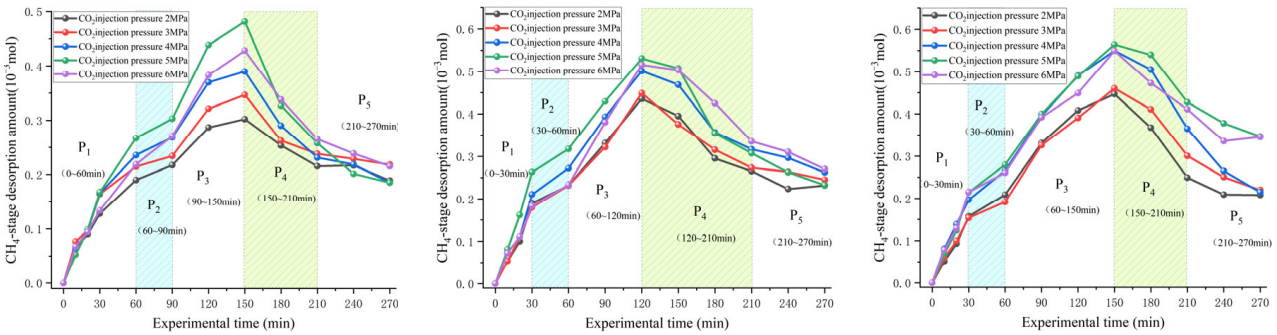

(**a**) (**b**) (**c**)

Figure 8. Time-varying characteristic curves of the desorption amount in the CH_4 desorption stage. (**a**) Anthracite; (**b**) Coking coal; (**c**) Long flame coal.

Figure 8 demonstrates that in the P_1 stage (anthracite: 0–60 min; coking coal and long-flame coal: 0–30 min), the desorption amount of CH_4 gas increased rapidly with experimental time. In the P_2 stage (anthracite: 60–90 min; coking coal and long-flame coal: 30–60 min), the upward trend shows a clear stage-wise slowdown. Conversely, in the

P_3 stage (anthracite: 90–150 min; coking coal: 60–120 min; long-flame coal: 60–150 min), the stage desorption amount of CH_4 gas again increased rapidly. By contrast, in the P4 stage (anthracite: 150–210 min; coking coal: 120–210 min; long-flame coal: 150–240 min), it decreased rapidly; and in the P_5 stage (anthracite and coking coal: 210–270 min; long-flame coal: 240–270 min), it tended to stabilize.

In the P_1 stage, when the connecting valve is opened and CO_2 gas enters the coal sample chamber, CO_2 first rapidly occupies the remaining adsorption sites because of the smaller size of CO_2 molecules compared to CH_4 molecules. Part of the CH_4 undergoes natural desorption and is expelled from the coal matrix due to the reduction in its partial pressure. Therefore, although the desorption amount of CH_4 gas increases rapidly with time in this stage, the cumulative desorption amount of CH_4 is still relatively small. Upon reaching the P_2 stage, pressure in the coal sample chamber tends to stabilize, the remaining adsorption sites within the coal are gradually occupied by CO_2 that has penetrated the coal matrix, CO_2 begins competitive adsorption with CH_4, and the replacement effect becomes dominant. Consequently, the stage desorption amount of CH_4 gas continues to rise, but more gradually. By the P_3 stage, the remaining adsorption sites in the coal have been completely occupied by CO_2 that has penetrated the coal. This stage includes not only the replacement effect of CO_2 on CH_4 but also the displacement effect, and both effects reach their peak, thus the stage desorption amount of CH_4 gas rises sharply. In the P_4 stage, with the decrease in the residual adsorbed CH_4 in the coal, the competitive adsorption between CO_2 and CH_4 gradually weakens, the replacement effect also diminishes, and the displacement effect becomes dominant. This leads to a continuous decline in the stage desorption amount of CH_4 gas. In the P5 stage, very little residual adsorbed CH_4 is left in the coal, the partial pressure of CH_4 is essentially stable, and the free CH_4 expelled from the coal under the displacement effect of CO_2 also stabilizes. Therefore, the stage desorption amount of CH_4 gas in this stage tends to stabilize.

The process of CO_2 gas displacement–replacement of CH_4 in coal seams can be divided into five stages, namely the following: (1) a stage of spontaneous CH_4 desorption caused by partial-pressure effects; (2) a replacement-dominated stage; (3) a stage where replacement and displacement act jointly; (4) a displacement-dominated stage; and (5) a stabilization stage.

4.1.2. Time-Varying Characteristics of Cumulative CH_4 Desorption Amount

A comparative analysis was performed on the cumulative CH_4 desorption at the end of the experiment under different CO_2 injection pressures, as shown in Figure 9.

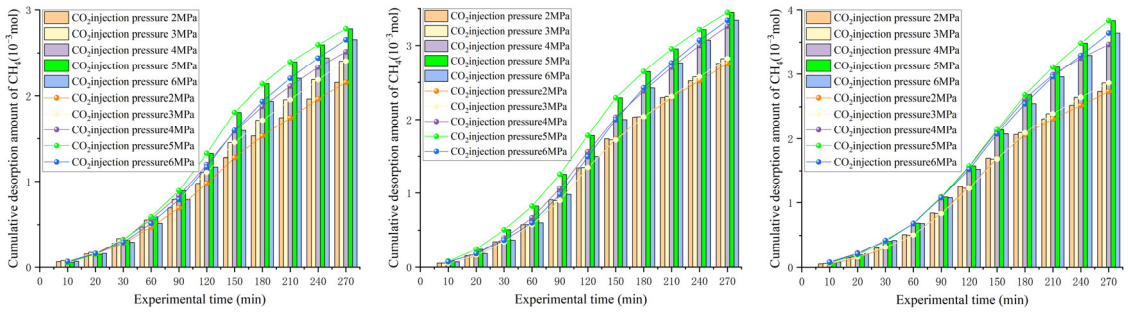

(**a**) (**b**) (**c**)

Figure 9. Time-varying characteristic curves of cumulative CH_4 desorption. (**a**) Anthracite; (**b**) Coking coal; (**c**) Long flame coal.

Figures 9 and 10 illustrate that at the end of the experiment, the cumulative desorption amount of CH_4 gas from the three coal samples increased with increasing CO_2 injection pressure and finally tended to be stable.

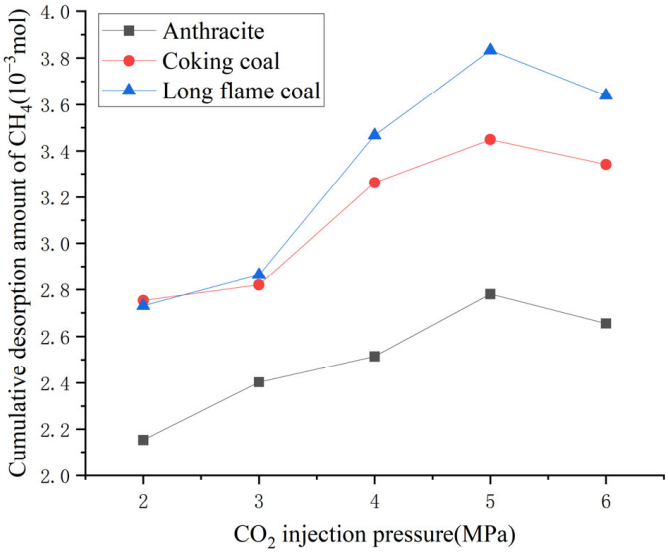

Figure 10. Relationship between cumulative CH_4 desorption and CO_2 injection pressure.

Table 3 summarizes that when the injection pressure of CO_2 gas increases from 2 to 5 MPa, the increase in the CH_4 desorption of long flame coal, coke, and anthracite is 29.12%, 25.26%, and 40.35%, respectively. When the injection pressure of CO_2 gas increases from 2 to 6 MPa, the increase in the CH_4 desorption of long flame coal is 23.30%, that of coke is 21.38%, and anthracite shows a 33.27% increase. This may be attributed to the higher difference in pressure, which leads to a faster desorption rate of CH_4 during the P_1–P_3 stage (0–150 min), resulting in a higher cumulative desorption amount. However, simultaneously, the rate of decrease in CO_2 partial pressure in the coal sample tank is also faster. By the time, the experiment reaches the P_4–P_5 stage (150–270 min), the partial pressure of CO_2 at 5 MPa injection pressure during this stage may be higher than that at 6 MPa, resulting in higher displacement and replacement efficiency under the condition of 5 MPa CO_2 injection pressure during this stage.

Table 3. The relationship between the increase rate of CH_4 desorption and CO_2 injection pressure.

CO_2 Injection Pressure/Mpa	Increase Rate of CH_4 Cumulative Desorption/%		
	Long Flame Coal	Coking Coal	Anthracite
3	4.86	2.43	11.59
4	26.96	18.50	16.75
5	40.35	25.26	29.12
6	33.27	21.38	23.30

4.1.3. Time-Varying Characteristics of the Displacement-to-Replacement Ratio

The effectiveness of CO_2 displacement and replacement is generally represented by the displacement/replacement ratio. That is, the higher the ratio, the higher the efficiency, and the better the effect. It is defined as the ratio of the amount of CO_2 adsorbed to the amount of CH_4 desorbed, and its calculation formula is represented as follows:

$$C = \frac{A_{CO_2}}{D_{CH_4}} \quad (7)$$

where C is the driving-out/displacement ratio; D_{CH_4} is the amount of CH_4 desorbed from the coal, mol; and A_{CO_2} denotes the amount of CO_2 adsorbed by the coal, mol.

Figure 11 illustrates that the displacement–replacement ratio increases with experimental time and then tends to stabilize. In the early stage of the experiment (stage T_1 in the figure), the displacement–replacement ratio rises rapidly with time. This is because after CO_2 invades coal, it reaches the pores via seepage and diffusion, quickly occupies the remaining adsorption sites, and competes with CH_4 for adsorption, thereby displacing adsorbed CH_4. During this stage, the diffusion coefficient of CO_2 is much higher than that of CH_4, thus the amount of CO_2 entering the coal far exceeds that of CH_4 exiting, leading to a rapid increase in the displacement–replacement ratio. In the mid-stage of the experiment (T_2), CO_2 completely occupies the remaining adsorption sites. The decrease in gas concentration gradients weakens diffusion while competitive adsorption becomes stronger. During this stage, not only replacement of adsorbed CH_4 by CO_2 occurs but also displacement of adsorbed CH_4 by CO_2 is observed. With the prolongation of time, the replacement effect gradually becomes dominant, causing the growth of the displacement–replacement ratio to slow down. In the late stage of the experiment (T_3), as adsorbed CH_4 continues to be displaced, the residual adsorbed CH_4 in the coal diminishes, and the replacement effect weakens accordingly. Therefore, the displacement–replacement ratio gradually levels off during this stage.

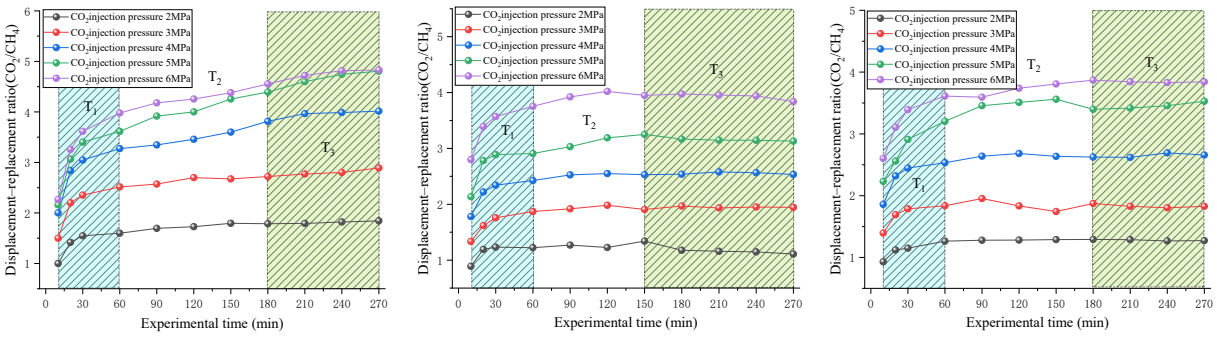

Figure 11. Time-varying characteristic curve of displacement–replacement ratio under different CO_2 injection pressure conditions. (**a**) Anthracite; (**b**) Coking coal; (**c**) Long flame coal.

4.2. Effect of CH_4 Equilibrium Pressure

The experiment utilized a controlled-variables method. Gaseous CO_2 was injected at 5 MPa under CH_4 equilibrium pressures ranging from 0.5 to 2.5 MPa and at a temperature of 30 °C. The CH_4 desorption per unit time was calculated, and the temporal evolution of CH_4 desorption stage was analyzed to uncover the time-varying characteristics of the displacement and replacement effects at varying CH_4 equilibrium pressures. This analysis aided in determining the applicability window for efficient CO_2-enhanced drainage of coal seam CH_4.

4.2.1. Time-Varying Characteristics of CH_4-Stage Desorption Amount

The relationships of the CH_4-stage desorption amount with displacement time and CO_2 injection pressure are shown in Figure 12.

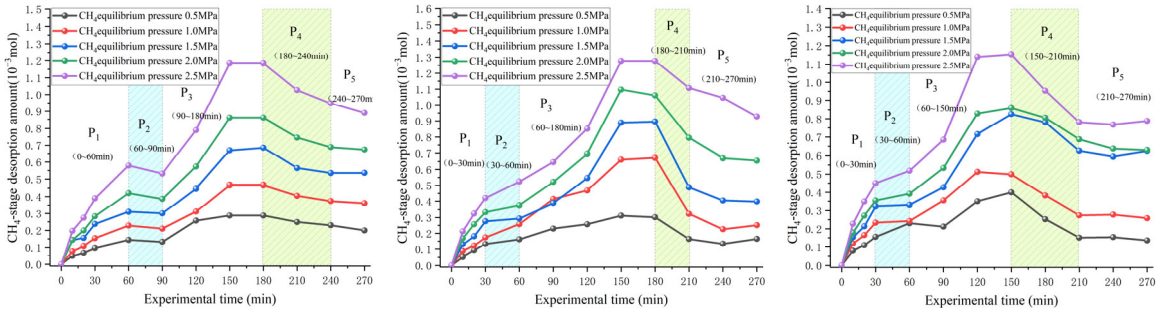

(**a**) (**b**) (**c**)

Figure 12. Time-varying characteristic curves of the desorption amount in the CH_4 stage. (**a**) Anthracite; (**b**) Coking coal; (**c**) Long flame coal.

Figure 12 illustrates that under different CH_4 equilibrium pressures, the CH_4 desorption stage exhibits trends that are highly consistent with those observed under varying CO_2 injection pressures. Similarly, based on the dominant mechanism in each stage, the entire process can be divided into five stages: (1) natural desorption of CH_4 induced by partial-pressure effects; (2) onset of the replacement effect; (3) coaction of replacement and displacement effects; (4) weakening of the replacement effect; and (5) displacement-dominated stage.

4.2.2. Time-Varying Characteristics of Cumulative CH_4 Desorption Amount

The cumulative amount of CH_4 desorbed at the end of the experiments under different CH_4 equilibrium pressure conditions was selected for comparative analysis, as shown in Figure 13.

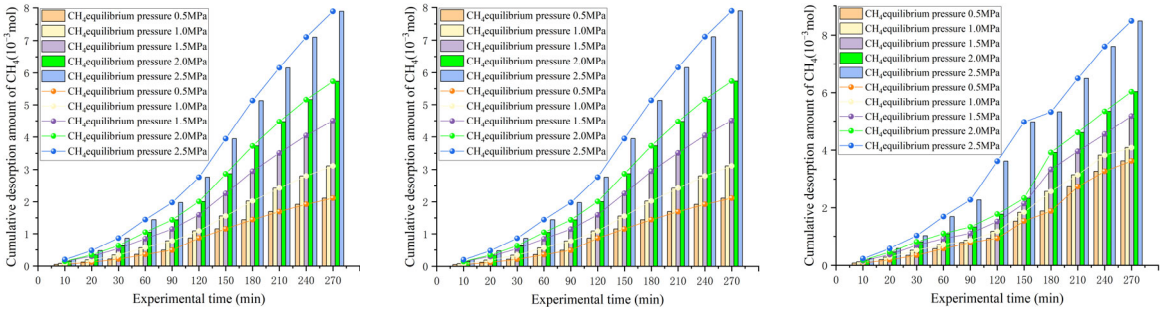

(**a**) (**b**) (**c**)

Figure 13. Time-varying characteristic curves of cumulative CH_4 desorption. (**a**) Anthracite; (**b**) Coking coal; (**c**) Long flame coal.

The curves shown in Figure 13 demonstrate that for all three coal samples, the cumulative CH_4 desorption first increases slowly and then rises rapidly with the progress of the experiment. Moreover, under different CH_4 equilibrium pressure conditions, the time-varying characteristics differ. That is, the higher the CH_4 equilibrium pressure, the shorter the initial slow-growth stage. The bar chart in Figure 13 further shows that the higher the CH_4 equilibrium pressure, the greater the cumulative CH_4 desorption. This is attributed to the fact that under the same CO_2 injection pressure, the CH_4 equilibrium pressure directly affects the initial CH_4 content within the coal and the extent of spontaneous desorption driven by partial pressure. With the increase in the CH_4 equilibrium pressure, the pressure difference relative to the CO_2 injection pressure decreases, thus weakening the partial-pressure effect after CO_2 injection. Therefore, the cumulative CH_4 desorption increases slowly at the beginning. Simultaneously, a higher initial CH_4 content enhances

the replacement effect and displacement effect, leading to a subsequent rapid increase in cumulative CH_4 desorption.

When the CH_4 equilibrium pressure is 0.5–1.5 MPa, the cumulative CH_4 desorption shows a slow increase during the first 90 min and then rises rapidly beyond 90 min. When the CH_4 equilibrium pressure is in the range of 2.0–2.5 MPa, it increases slowly during the first 30 min and then rises rapidly thereafter. Thus, the higher the CH_4 equilibrium pressure, the shorter the period of spontaneous CH_4 desorption, and the longer the period dominated by replacement and displacement effects.

4.2.3. Time-Varying Characteristics of the Displacement-to-Replacement Ratio

Figure 14 exhibits that the displacement–replacement ratio rises rapidly with experimental time and then levels off, which is consistent with the conclusions mentioned above. Moreover, the displacement–replacement ratio decreases with increasing CH_4 equilibrium pressure. As shown in Table 4, the increase in the CH_4 equilibrium pressure from 0.5 to 2.5 MPa leads to a decrease in the displacement–replacement ratios for the three coal samples at 270 min: 72.83% for long-flame coal, 80.14% for coking coal, and 70.48% for anthracite. This result indicates that the larger the pressure difference between the CO_2 injection pressure and the CH_4 equilibrium pressure, the more effective the displacement–replacement process.

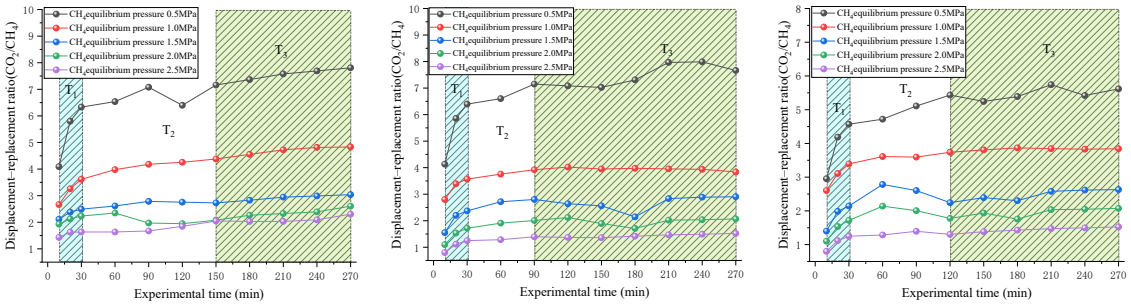

Figure 14. Time-varying characteristic curve of displacement–replacement ratio under different CH_4 equilibrium pressure conditions. (**a**) Anthracite; (**b**) Coking coal; (**c**) Long flame coal.

Table 4. Relationship between CH_4 pressure difference and displacement–replacement decline.

Pressure Difference/Mpa	Decline of Displacement and Displacement Ratio/%		
	Long Flame Coal	Coking Coal	Anthracite
0.5	26.44	26.34	11.52
1	42.01	47.59	24.10
1.5	60.29	60.36	52.28
2	72.83	80.14	70.48

5. Conclusions

The process by which CO_2 gas displaces and replaces CH_4 in coal seams can be divided into five stages: spontaneous CH_4 desorption induced by partial-pressure effects; a replacement-effect dominated stage; a stage where replacement and displacement effects act jointly; a displacement-effect dominated stage; and a steady stage.

Under the conditions of different CH_4 equilibrium pressures, the variation trend of CH_4 gas desorption at different stages is highly consistent with that under different CO_2 injection pressures. Moreover, both of them show a rapid increase and then decrease with time and finally stabilizes. The inflection point of the curve can be used as the basis for

dividing each stage in the entire process of CO_2 displacement and replacement of coal seam CH_4.

For all three coal samples, the cumulative CH_4 desorption increased with increasing CO_2 injection pressure and eventually stabilized. However, the effect weakened when the CO_2 injection pressure exceeded 5 MPa. This weakening may have been caused by the dynamic changes in the partial pressure of CO_2.

The displacement–replacement ratio decreases with increasing CH_4 equilibrium pressure. When the CH_4 equilibrium pressure rises from 0.5 to 2.5 MPa, the displacement–replacement ratio at 270 min for the three coal samples decreases by 72.83% for long-flame coal, 80.14% for coking coal, and 70.48% for anthracite. This indicates that the larger the pressure difference between the CO_2 injection pressure and the CH_4 equilibrium pressure, the more effective the displacement–replacement process.

Author Contributions: Data curation, J.H.; Writing—original draft preparation, J.H. and H.W.; Writing—review and editing, S.W.; Investigation, X.Z.; Supervision, Z.L. All authors have read and agreed to the published version of the manuscript.

Funding: This research was funded by Shaanxi Provincial Department of Human Resources and Social Security, Postdoctoral Foundation of Shaanxi Province, China, grant number 2023BSHEDZZ2291 and Shaanxi Provincial Department of Science and Technology, Youth Fund of Shaanxi Province, China, grant number 2024JC-YBQN-0532.

Data Availability Statement: The original contributions presented in the study are included in the article, further inquiries can be directed to the corresponding author.

Conflicts of Interest: The authors declare no conflict of interest.

References

1. Wang, S. On the status of coal as a primary energy source in China and green mining. *China Coal* **2020**, *46*, 11–16. [CrossRef]
2. Ge, S.; Liu, S.; Fan, J.; Zhao, J.; Teng, T. Key technological system for low-carbon modern coal-based energy development. *J. China Coal Soc.* **2024**, *49*, 2949–2972.
3. Wang, F.; Kobina, F. The Influence of Geological Factors and Transmission Fluids on the Exploitation of Reservoir Geothermal Resources: Factor Discussion and Mechanism Analysis. *Reserv. Sci.* **2025**, *1*, 3–18. [CrossRef]
4. Wu, J.; Ansari, U. From CO_2 Sequestration to Hydrogen Storage: Further Utilization of Depleted Gas Reservoirs. *Reserv. Sci.* **2025**, *1*, 19–35. [CrossRef]
5. Yuan, L.; Jiang, Y.; Wang, K.; Zhao, X.; Hao, X.; Xu, C. Scientific considerations for precise development and utilization of resources in China's closed/abandoned mines. *J. China Coal Soc.* **2018**, *43*, 14–20. [CrossRef]
6. Wang, E.; Zhang, G.; Zhang, C.; Li, Z. Research progress and prospects of theory and technology for prevention and control of coal and gas outbursts in China. *J. China Coal Soc.* **2022**, *47*, 297–322. [CrossRef]
7. Su, X.; Song, J.; Guo, H.; Pu, H.; Liu, X.; Han, Y.; Zhang, S.; Li, X.; Yu, S. Mechanisms and key technologies for enhancing coal mine gas drainage productivity. *Coal Sci. Technol.* **2020**, *48*, 1–3. [CrossRef]
8. Liu, S.; Zhu, C.; Lin, B.; Liu, T. Effects of spatial distribution patterns of hydraulic slotting on pressure relief and permeability enhancement in coal seams. *J. Min. Saf. Eng.* **2020**, *37*, 983–990. [CrossRef]
9. Wong, S.; Macdonald, D.; Andrei, S. Conceptual economics of full scale enhanced coalbed methane production and CO_2 storage in anthracitic coals at South Qinshui basin, Shanxi, China. *Int. J. Coal Geology* **2010**, *82*, 280–286. [CrossRef]
10. Yi, M.; Wang, L.; Cheng, Y.; Wang, C.; Hu, B. Calculation of gas concentration-dependent diffusion coefficient in coal particles: Influencing mechanism of gas pressure and desorption time on diffusion behavior. *Fuel* **2022**, *320*, 123973. [CrossRef]
11. Wen, H.; Hao, J.; Ma, L.; Ren, L.; Wei, G.; Zheng, X. Study on the adsorption characteristics of coal samples before and after liquid CO_2 immersion–dissolution. *J. Xi'an Univ. Sci. Technol.* **2022**, *42*, 397–404. [CrossRef]
12. Yang, H.; Wei, C.; Wang, Z.; Yang, T. Numerical simulation of underground gas injection to displace coalbed methane based on multi-physics coupling. *J. China Coal Soc.* **2010**, *35* (Suppl. S1), 109–114. [CrossRef]
13. Yang, H.; Zhang, T.; Wang, Z.; Zhao, C. Experimental study on nitrogen injection into coal seams to displace methane and promote gas drainage. *J. China Coal Soc.* **2010**, *35*, 792–796. [CrossRef]
14. Yang, H.; Feng, C.; Chen, L. Analysis of displacement–driving effects and their transformation mechanisms in nitrogen injection simulation experiments in coal seams. *J. China Coal Soc.* **2016**, *41*, 2246–2250. [CrossRef]

15. Liang, W.; Zhang, B.; Li, L.; He, W. Theoretical and experimental study on energy injection (with CO_2 as an example) for modified displacement extraction of CH_4. *J. China Coal Soc.* **2018**, *43*, 2839–2847. [CrossRef]
16. Liang, W.; Wu, D.; Zhao, Y. Experimental study on CO_2 displacement of coal seam CH_4. *Chin. J. Rock Mech. Eng.* **2010**, *29*, 665–673.
17. Wang, L. Experimental Study on Gas-Injection Displacement of CH_4 in Deep Coal Seams and Post-Displacement Characteristic Traces. Ph.D. Thesis, China University of Mining and Technology, Xuzhou, China, 2013.
18. Wang, L.; Wang, Z.; Xu, S.; Zhou, W.; Wu, J. A field investigation of the deformation of protected coal and its application for CBM extraction in the Qinglong coalmine in China. *J. Nat. Gas Sci. Eng.* **2015**, *27*, 367–373. [CrossRef]
19. Yue, G.; Wang, Z.; Kang, B. Time-varying characteristics of the gas diffusion coefficient of coal in low-temperature environments. *China Saf. Sci. J.* **2014**, *24*, 107–112. [CrossRef]
20. Sun, K.; Liang, B.; Pan, Y. Study on the productivity-enhancement mechanism of coalbed methane extraction by gas injection under fluid–solid coupling. *Sci. Technol. Eng.* **2006**, *6*, 802–806, 813.
21. Zhang, W.; Tai, Y. Numerical simulation of coalbed methane production by injection wells. *J. Liaoning Tech. Univ. (Nat. Sci. Ed.)* **2009**, *28*, 291–298.
22. Wu, S.; Zheng, A. A three-dimensional multicomponent flow model for gas-injection displacement of coalbed methane. *Nat. Gas Geosci.* **2007**, *18*, 580–583.
23. Zheng, A.; Wang, X.; Liu, D. Numerical simulation study of gas-injection displacement of coalbed methane. *Pet. Drill. Tech.* **2006**, *31*, 55–57.
24. Mei, H.; Zhang, M.; Li, M.; Sun, L.; Dong, H.; Gu, H. Flow equation considering dispersion during the gas-drive process. *Nat. Gas Ind.* **2004**, *24*, 97–99.
25. Wen, H.; Fan, S.; Ma, L.; Guo, J.; Wei, G.; Hao, J. Engineering practice of promoting gas drainage in low-permeability coal seams using low-pressure liquid CO_2 underground. *J. Xi'an Univ. Sci. Technol.* **2018**, *37*, 530–537. [CrossRef]
26. Wen, H.; Hao, J.; Ma, L.; Zheng, X. Experimental Study on Replacing Coal Seam CH_4 with CO_2 Gas. *ACS Omega* **2022**, *7*, 1395–1403. [CrossRef]
27. Wei, G.; Wen, H.; Deng, J.; Li, Z.; Fan, S.; Lei, C.; Liu, M.; Ren, L. Enhanced coalbed permeability and methane recovery via hydraulic slotting combined with liquid CO_2 injection. *Process Saf. Environ. Prot.* **2021**, *147*, 234–244. [CrossRef]
28. *DIN EN ISO 12213-2-2010*; Natural Gas. Calculation of the Compression Factor. Part 2. Algebraic Analysis of Molar Calculations (ISO 12213-2-2006). German Version EN ISO 12213-2-2009. German Institute for Standardisation: Berlin, Germany, 2010.

Disclaimer/Publisher's Note: The statements, opinions and data contained in all publications are solely those of the individual author(s) and contributor(s) and not of MDPI and/or the editor(s). MDPI and/or the editor(s) disclaim responsibility for any injury to people or property resulting from any ideas, methods, instructions or products referred to in the content.